Solar Cells, *23* (1988) 1 - 17

CdTe JUNCTION PHENOMENA

RICHARD H. BUBE

Department of Materials Science and Engineering, Stanford University, Stanford, CA 94305 (U.S.A.)

(Accepted September 17, 1987)

Summary

Five main areas of research on CdTe junction phenomena are reviewed in this paper: (1) the effect of surface etching and stoichiometry on the properties of Schottky barriers and heterojunctions with CdS and indium tin oxide (ITO) formed on p-type CdTe crystal; (2) the major junction transport models applicable to CdS/CdTe, CdS/ZnCdTe, ZnO/CdTe and ITO/CdTe junctions; (3) the deposition and control of the properties of p-type CdTe films using close-spaced vapor transport and the characteristics of CdS/CdTe junctions prepared with these films; (4) the successful doping of p-type CdTe films during growth by ion-beam doping methods; and (5) methods of preparing low-resistivity contacts to p-CdTe.

---

1. Introduction

Modern interest in CdTe dates back to 1947 when Frerichs [1] grew single crystals of CdTe from the vapor phase reaction of cadmium and tellurium in the presence of hydrogen. de Nobel's [2] exploratory work on the effects of the deviation from stoichiometry in CdTe laid the foundations for an understanding of the crystal growth of CdTe from the melt with well-defined electrical properties. Because of the excellent match of its band gap with the solar spectrum and the possibility of preparing CdTe in both high conductivity n and p type, it was suggested early on as a possible candidate for a solar cell material [3, 4]. When it was recognized that the Cu_xS/CdS heterojunction did not possess the stability required of a commercial solar cell system, it was natural to investigate the CdTe/CdS system, with the II–VI compound p-CdTe taking the place of the p-type Cu_xS. Several extensive reviews of the properties of CdTe have been published [5 - 7] as well as a review of CdTe solar cells [8].

CdTe solar cells with an efficiency approaching 10% or higher have been made as heterojunctions, homojunctions, buried homojunctions and metal/insulator/semiconductor (MIS) junctions, using single-crystal CdTe

0379-6787/88/$3.50

TABLE 1

Representative high efficiency CdTe solar cells

Cell	*Open-circuit voltage* (V)	*Short-circuit current* (mA cm^{-2})	*Solar efficiency* (%)	*Reference*
Efficiency greater than 10%				
CdTe homojunction: p-CdTe deposited by CSVT on large-grain n-CdTe	0.82	21	10.7	9, 10
n-ITO/p-CdTe heterojunction: electron beam evaporated ITO on single-crystal p-CdTe	0.81	20	10.5	11
n-CdS/p-CdTe heterojunction[a]: both layers deposited by CSVT	0.75	17	10.5	12
n-CdS/p-CdTe buried homojunction: CdS deposited by CVD[b] on single-crystal CdTe	0.67	20	11.7	13, 14
n-CdS/p-CdTe heterojunction[a] formed by CSVT deposition of p-CdTe on vacuum-evaporated n-CdS	0.75	22	10.5	15
n-ITO/p-CdTe buried homojunction formed by reactive deposition of ITO on single-crystal CdTe	0.89	20	13.4	16
n-CdS/p-CdTe heterojunction[a] formed by electrodeposition of CdTe on CdS deposited by spray pyrolysis	0.74	22	10.4	17
n-CdS/p-CdTe buried homojunction[a]: both layers deposited by screen printing	0.75	22	12.8	18 - 22
n-CdS/p-$Cd_{0.9}Hg_{0.1}Te$ heterojunction[a]: both layers deposited by electrodeposition	0.62	27	10.6	23
Efficiency less than 10%				
n-CdS/CdTe/p-ZnTe n-i-p cell[a] with CdS deposited by spray pyrolysis, CdTe by electrodeposition, ZnTe by evaporation	0.69	22	9.4	17
MIS Au/n-CdTe cell[a] deposited by electrodeposition	0.72	19	8.7	24
n-CdS/p-CdTe heterojunction[a]: both layers deposited by electrodeposition	0.73	20	9.4	25
n-ITO/p-CdTe buried homojunction: n-ITO sputtered on single-crystal CdTe	0.82	14.5	8.0	26
n-ZnO/p-CdTe heterojunction: n-ZnO deposited by spray pyrolysis on single-crystal CdTe	0.54	19.5	8.8	27
n-CdS/p-CdTe heterojunction: vacuum-evaporated CdS on single-crystal CdTe	0.63	16	7.9	28
n-CdS/p-CdTe heterojunction: n-CdS deposited by spray pyrolysis on single-crystal CdTe	0.53	16	6.5	29

[a] An all thin film cell.

[b] Chemical vapor deposition.

or thin film CdTe produced using a variety of deposition techniques, including close-spaced vapor transport (CSVT), screen printing and electrodeposition. Table 1 summarizes the major types of CdTe-based solar cells.

In this paper, we review some of the research dealing with CdTe surface and interface effects on junction properties, the results of attempts to model heterojunction transport for a few cases where sufficient data are available to allow such modelling, basic phenomena involved in the CSVT deposition of p-CdTe films, ion-beam doping of p-CdTe films deposited from the vapor phase and properties of low-resistance contacts to p-type CdTe. These are some of the topics of major interest to our research program on CdTe-based solar cells at Stanford over the past 15 years; of necessity, they represent only a partial perspective even on the topics discussed.

2. Surface effects on metal/CdTe junctions and CdTe heterojunctions

Surfaces of single-crystal CdTe are commonly etched to remove damage due to polishing; a usual etch for this purpose is bromine in methanol (Br_2–MeOH). Werthen and coworkers [11, 30 - 33] have examined in some detail the nature of the surface conditions and their effect on Schottky barriers and heterojunctions formed with indium tin oxide (ITO) or CdS.

The cleavage of CdTe produces a stoichiometric surface (determined using X-ray photoemission spectroscopy (XPS) analysis), whereas etching with Br_2–MeOH leaves a tellurium-rich surface. If the etched surface is heated in hydrogen (425 °C for 5 min), again a stoichiometric surface is obtained, presumably as a result of thermal cleaning of the surface.

The properties of junctions formed on these surfaces are very sensitive to the presence or absence of stoichiometry. They are also sensitive to a lesser extent to the specific crystal orientation of the surface. The junction properties corresponding to a surface heated in hydrogen after etching are essentially the same as those corresponding to a cleaved surface that has never been etched; we refer to both of them as stoichiometric surfaces.

Figure 1 shows the variation in current with voltage under illumination for polished and etched (PE) and polished, etched and hydrogen-heated (PEH) Schottky barriers formed by evaporating chromium onto the CdTe. The results indicate both a major effect associated with the stoichiometry of the CdTe surface and secondary effects associated with the crystallographic surface orientation. The presence of the excess tellurium on the non-stoichiometric surface can be shown to result in a reduction in the Cr/CdTe barrier height from 0.87 to 0.65 eV. This decrease in the barrier height results in a large increase in the reverse saturation current density J_0 which in turn causes the reduction in the open-circuit voltage under illumination shown in Fig. 1.

The barrier heights of Schottky barriers formed on the non-stoichiometric surfaces are found to be independent of the work function of the metal and to be all of the order of 0.65 eV for gold, chromium, aluminum

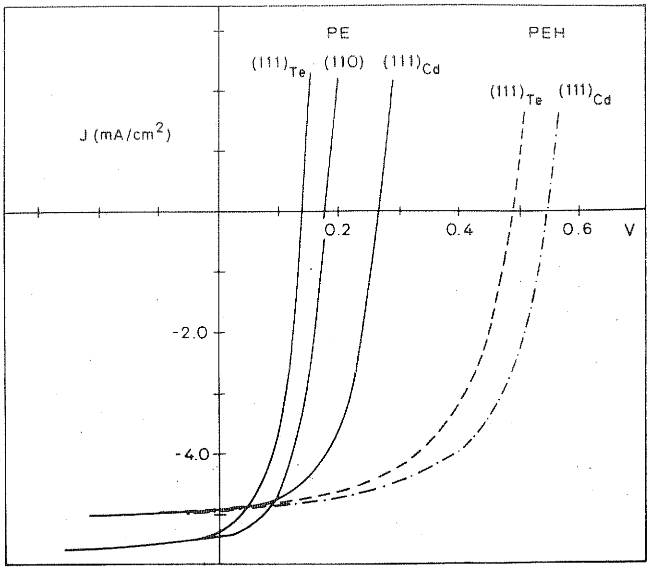

Fig. 1. Light *J–V* characteristics of Cr/CdTe junctions formed on polished and etched (PE) and polished, etched and heat treated (PEH) surfaces of different orientations (see ref. 32).

and indium. For the stoichiometric surface, however, the barrier height is a function of the metal work function, increasing from 0.65 eV for gold to about 1.0 eV for aluminum or indium. Similar effects were found for CdS/CdTe heterojunctions formed by vacuum evaporation of CdS onto stoichiometric and non-stoichiometric surfaces, the open-circuit voltage for the former being several tenths of a volt larger than for the latter.

Somewhat unexpected results were obtained when ITO/CdTe junctions were prepared on stoichiometric and non-stoichiometric surfaces by electron beam evaporation of the ITO. In order to produce optically transparent ITO films, it was necessary to subject the deposited ITO/CdTe structure to a heat treatment in air (225 °C for 2 min) in order to cause the amorphous ITO film to crystallize. This post-deposition heat treatment caused an increase in J_0 of three orders of magnitude for the ITO/CdTe formed with stoichiometric CdTe surfaces but an increase only of one order of magnitude for the non-stoichiometric surfaces. In this specific case, therefore, it appears that the excess tellurium on the etched surface actually protects the junction during the heat treatment in air.

By reducing the doping of the p-CdTe in the ITO/CdTe junctions, a considerable increase in the open-circuit voltage from 0.41 V for a hole concentration of 10^{17} cm^{-3} to 0.81 V for a hole concentration of 10^{15} cm^{-3} could be achieved, apparently because of increased diode factor values at constant J_0 as the recombination shifted from the interface to the depletion region. It was, in fact, this lowest-doped CdTe that yielded the highest solar efficiency of 10.5% listed in Table 1.

d and etched
ntations (see

er height is
V for gold
found for
CdS onto
uit voltage
ter.
Te junctions
es by elec-
transparent
Te structure
amorphous
caused an
ormed with
f magnitude
e, it appears
the junction

e junctions,
r a hole con-
f 10^{15} cm^{-3}
or values at
he depletion
highest solar

An increase in the open-circuit voltage from 0.45 to 0.55 V was also observed for Cr/CdTe Schottky barriers formed after the CdTe had been exposed to air at room temperature for several hours. The barrier height was unchanged by the exposure to air but the value of J_0 was reduced by a factor of 5, indicating that the oxide formed on the CdTe and identified as TeO_2 by XPS was causing a useful MIS junction. Such formation of TeO_2 on CdTe is a non-equilibrium process since careful investigation of the thermal oxidation of CdTe by Wang *et al.* [34] showed that $CdTeO_3$ is the stable native oxide.

The detailed modeling of the above phenomena is made somewhat more complex by the recognition of the fact that heat treatment of p-CdTe:P crystals in hydrogen causes a decrease in the hole density near the surface. Nishimura and Bube [35] showed that heat treatment of p-CdTe:P crystals in hydrogen at temperatures between 310 and 475 °C decreases the hole density near the surface by as much as a factor of 25, corresponding to an approximately exponential acceptor density profile. The decrease in the hole density caused by heating for 80 min in hydrogen at 340 K, for example, can be almost totally prevented by the deposition of CdS on the CdTe during this period. A number of possible mechanisms might individually or cooperatively be responsible for this behavior: (1) out-diffusion of phosphorus acceptors from the CdTe, (2) in-diffusion of cadmium vacancies from the surface, and (3) out-diffusion of excess tellurium from the bulk to the surface to form anti-site defects.

3. Heterojunction transport models

In order to carry out any meaningful modeling of junction transport, it is necessary (as a minimum) to have a reliable family of forward current (J) *vs.* voltage (V) curves as a function of temperature in the dark, and a similar family of short-circuit current (J_{sc}) *vs.* open-circuit voltage (V_{oc}) curves (measured by varying the light intensity) as a function of temperature. Then the simplest indications of junction transport are the following: (1) the identification of the type of transport according to whether the slopes of the J–V curves vary as $1/T$, thus indicating a constant A factor ($J = J_0 \exp(qV/AkT)$) as expected for such junction processes as diffusion, bulk recombination or interface recombination, or whether the slope is essentially temperature independent, thus indicating a constant (or nearly constant) a ($J = J_0 \exp(aV)$) as expected for junction transport dominated by tunneling; (2) the specific magnitude of A or a, and whether a is strictly or only almost temperature independent; (3) the comparison of J–V in the dark with J_{sc}–V_{oc} in the light, which indicates whether the junction transport process changes under illumination. If, in addition it is desired to model the photocurrent collection process, it is necessary to have also (as a minimum) the spectral response of the short-circuit current measured for different applied biases in order to determine the importance of bulk recombination and interface recombination.

An early evaluation of the CdS/CdTe heterojunction solar cell was carried out by Mitchell *et al.* [28]. These cells were made by vacuum evaporation of CdS onto single-crystal p-CdTe, and their parameters are listed in Table 1. A comparison with what might be expected from ideal recombination-controlled transport indicated that the major loss was in the open-circuit voltage, which was only 0.63 V, compared with the theoretically expected value of 0.90 V, corresponding to a value of J_0 (about 10^{-8} A cm^{-2}) that was two orders of magnitude larger than that predicted for simple recombination-controlled transport. Above room temperature, the J–V curves indicated a constant value of $A = 1.89$, suggesting that junction currents were controlled by recombination in the depletion region at these higher temperatures. In this temperature range, J_0 was thermally activated with an activation energy of $\Delta E = 0.60$ eV, in apparent agreement with equating the theoretical diffusion voltage of 1.18 V for the junction with $A\Delta E$. Below room temperature, however, an essentially constant value of $a = 21.9\ \text{V}^{-1}$ was reported, indicating that transport was controlled by tunneling in this temperature range. The temperature dependence of J_0 is shown in Fig. 2. Since the hole density of $3.2 \times 10^{16}\ \text{cm}^{-3}$ in the CdTe corresponds to a depletion layer too wide to allow single-step tunneling, it was proposed that multistep tunneling might be invoked after the model of Riben and Feucht [36, 37] which would call for about 30 tunneling steps to fit the data.

Characteristics of these results persist in later work as well. The open-circuit voltages of experimental CdTe junctions are often found to be much smaller than the values listed for the cells described in Table 1, and fine tuning of the junction deposition processes is required to make the improvements in a number of solar cell parameters which result in a higher overall solar efficiency. Evidence for tunneling currents is frequently found even though the bulk acceptor density is known to be too small to allow such tunneling in a one-step model. Below we give some examples of these phenomena.

Fortmann *et al.* [38] have proposed a model for one cause of the reduced open-circuit voltage frequently found for CdS/CdTe junctions. They showed that the open-circuit voltage of CdS/CdTe heterojunction solar cells was at a maximum when the carrier densities in the CdS and the CdTe are approximately equal. For thin film CdS/CdTe/graphite cells in which the CdS was vacuum evaporated onto a CdTe film previously deposited by hot-wall vacuum evaporation (HWVE), control of the carrier density in the CdS was achieved by varying the substrate temperature. When the carrier density in the CdS was much less than in the CdTe, the open-circuit voltage was 0.48 V; this was increased to 0.67 V by making the two carrier densities equal. The effect was even more dramatic in CdS/CdTe cells prepared by vacuum evaporation of CdS onto single-crystal CdTe; an open-circuit voltage of 0.52 V found for a carrier density in the CdS less than that in the CdTe became 0.80 V when the carrier densities were made equal and then decreased again to 0.74 V when the carrier density in the CdS was much larger than in the CdTe.

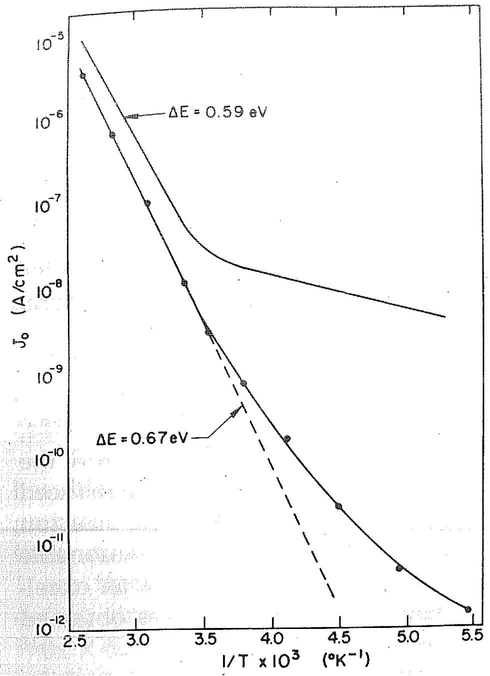

Fig. 2. Reverse saturation current as a function of reciprocal temperature for CdS/CdTe heterojunctions (see ref. 66): upper curve, CdS film vacuum-evaporated onto a single-crystal CdTe substrate (according to the data of Mitchell [28]); lower curve, CdS film vacuum-evaporated onto a CdTe film deposited by close-spaced vapor transport on graphite (according to the data of Anthony [49]).

At first it may seem somewhat surprising that equal sharing of the depletion width between the CdS and the CdTe should be the condition for maximum open-circuit voltage. Fortmann *et al.* argued, however, that junction transport was being controlled by a level lying 0.45 eV below the conduction band of CdTe, which was identified by measurements of the extrinsic photoresponse of CdS/CdTe junctions. The model based on the effects of this level on the junction transport, which successfully described the observed effects, involved two recombination paths: (1) depletion-layer recombination in the CdTe through the 0.45-eV level, which dominates when the electron density in the CdS is much larger than the hole density in the CdTe, and (2) tunneling of electrons from the CdS conduction band to the 0.45-eV level in the CdTe, followed by recombination, which dominates in other cases. The total junction current is minimized with respect to these two current mechanisms when the carrier densities in the two materials are equal. Whether this interpretation has universal applicability to CdS/CdTe cells remains to be seen.

The observation of a junction current that can be described with apparent success by a thermally assisted tunneling model, even when the bulk acceptor density in the CdTe is much too low to allow such tunneling in a conventional band-to-band or band-to-interface tunneling model, is common to several different systems such as CdS/CdTe [28] mentioned above, ZnO/CdTe [27], CdS/ZnCdTe [39], ZnO/InP [40], n-GaInAs/p$^+$-GaAs [41, 42] and CdS/CuInSe$_2$ [43].

An example of a CdTe-based junction system in which tunneling dominates the *J–V* curves over the whole temperature range is given by Aranovich *et al.* [27] who prepared ZnO/CdTe heterojunction cells by spray pyrolysis deposition of ZnO onto single-crystal p-CdTe substrates. Although cells with an efficiency of 8.8% could be fabricated, this required careful control of the CdTe substrate temperature during ZnO deposition and a post-deposition heat treatment in hydrogen to control the conductivity of the ZnO. The open-circuit voltage remained at the low value of 0.54 V in spite of an expected junction barrier height of 1.35 eV. Even though there is a very large (28%) lattice mismatch between ZnO and CdTe, quantum efficiencies of 80% were achieved without applied bias, and the potential problems of interface states were experienced only in the reduced open-circuit voltage. The application of the model of Padovani and Stratton [44, 45] for thermally assisted tunneling in Schottky barriers, reasonable in this case because of the high electron density in the ZnO, gave an excellent interpretation of the slightly temperature-dependent a values obtained from dark *J–V* curves corresponding to an acceptor density of 2.5×10^{18} cm^{-3}, in spite of a measured bulk hole density of 10^{17} cm^{-3}. A plot of the suitably temperature-corrected J_0 *vs.* a, according to the model, yielded a straight line over five orders of magnitude with an activation energy of 1.35 eV, in good agreement with the junction barrier height, as predicted from the model. Evidence was found that deep acceptor-like levels lying 0.86 eV above the valence band in the bulk of the CdTe shrink the depletion-layer width near the top of the barrier and give rise to the large tunneling currents observed. The forward current was observed to saturate in a plot of ln J *vs.* V when sufficient forward bias was applied to raise the Fermi level above the level associated with these deep levels.

Another example of *J–V* curves dominated by tunneling is given by Peters [39], who reported similar results for CdS/ZnCdTe heterojunction cells prepared by vacuum evaporation of CdS onto single-crystal Zn$_{0.3}$Cd$_{0.7}$Te substrates. The model of Padovani and Stratton was again observed to give a good fit to the slight temperature dependence of a, obtained from the dark ln J *vs.* V curves, provided that an acceptor density of 1.5×10^{19} cm^{-3} was assumed (the measured bulk hole density was 10^{16} cm^{-3}). It was suggested that a large density of negatively charged interface states is formed upon junction formation which increases the tunneling probability for holes. A plot of J_0, suitably temperature corrected according to the model, as a function of a, gives a straight line over five orders of magnitude with an activation energy of 1.04 eV for a junction made on a ZnCdTe substrate after Br$_2$–MeOH etching and heat treatment in hydrogen for an optimum time to achieve surface stoichiometry; this activation energy is in reasonable agreement with the expected value of the junction diffusion potential on the ZnCdTe side of the junction for this sample.

Two other interesting properties of these CdS/ZnCdTe junctions are worth noticing. The magnitude of the tunneling current, as indicated by an increase in J_0, is increased both by illumination (from 5×10^{-7} to 5×10^{-6} A cm^{-2} from measurements of J_{sc} *vs.* V_{oc} for a CdS/$Zn_{0.3}Cd_{0.7}Te$ junction, with the increase persisting after cessation of illumination) and by an increase in the concentration of zinc in the ZnCdTe solid solution (from 10^{-8} A cm^{-2} for $x = 0$ to 10^{-6} A cm^{-2} for $x = 0.3$). The effect of illumination on increasing J_0 is consistent with a model of photogenerated electrons being trapped by the interface states, thus increasing tunneling currents further. The increase in J_0 with increasing x in $Zn_xCd_{1-x}Te$ may be tentatively attributed to an increase in the interface density with increasing distortion as x increases to values of about 0.50.

One other variation in the properties of CdTe-based heterojunctions has been discussed by Courreges *et al.* [26]. ITO/CdTe junctions were prepared by sputtering ITO onto p-CdTe single-crystal substrates. Under these conditions it was found that a surface layer of p-type CdTe, about 1 μm thick, was converted to n type as a consequence of changes in the defect structure thermally induced by sputtering. Sputtering voltages between 800 and 1600 V had similar effects. The result was a buried homojunction of the type n$^+$-ITO/n-CdTe/p-CdTe. This junction had a much higher V_{oc} (0.82 V) than the corresponding ITO/CdTe heterojunction (0.62 V), and solar efficiencies of at least 8% were achievable. The n-CdTe layer, however, was unstable and showed both aging at 300 K and thermal degradation effects as the homojunction converted to the heterojunction. Analogous effects were reported for sputtered ITO/InP junctions [46]. In an investigation of the effects of sputtering damage on single-crystal p-type CdTe, Chien [47] has shown that the ion-energy threshold for damage effects is slightly below 100 V.

4. Close-spaced vapor transport deposition of thin film CdTe

The CSVT method of film deposition has been applied to CdTe by several different investigators [15, 48, 49]. A high density graphite source and substrate blocks are heated independently by quartz–halogen lamps with a spacing between source and substrate of the order of 1 mm.

CdTe homojunctions have been prepared by the deposition of a film of CdTe by CSVT onto a single-crystal substrate of opposite carrier type with some success [9, 10]. Early exploratory attempts to prepare CdS/CdTe heterojunctions by CSVT [50 - 52] were succeeded by major improvements developed by Tyan and Perez-Albuerne [12]; the parameters are given in Table 1. Both CdS and CdTe layers were deposited by CSVT to form a cell with the structure, glass/In_2O_3/0.1 μm CdS/4 μm CdTe/Au. It was reported that a small concentration of oxygen introduced during the deposition enhances the p-type character of the CdTe film and ensures a shallow junction between the CdS and the CdTe rather than a less desirable buried junction in the CdTe.

The use of CSVT for the deposition of CdTe films and the electrical properties of the films deposited were investigated in detail by Anthony and coworkers [48, 49]. A diffusion-limited transport model for the deposition process was indicated. Parallel growths in helium and in hydrogen indicated the relative ineffectiveness of hydrogen as a transport agent for CdTe.

Films of CdTe deposited by CSVT on glass, single-crystal CdTe and graphite substrates were all p type with maximum hole densities of 10^{16} cm^{-3} being achievable without intentional doping of the films. Careful investigation indicated that the hole density in the films was controlled neither by dopant transport from the source (hole densities obtained for undoped sources being as high as for strongly doped sources) nor by impurities in the CSVT system. The magnitude of the hole density in the films did not vary either with the nature or density of the acceptor dopant in the source or with the growth rate but did increase exponentially with the substrate temperature. A model involving only the thermal creation of intrinsic acceptor defects, including self-compensation effects due to other intrinsic defects, was constructed to describe the dependence of the hole density on the substrate temperature.

CdS/CdTe/graphite heterojunction solar cells were prepared by vacuum evaporation of CdS on CdTe films deposited on graphite by CSVT; the most efficient cell showed $V_{oc} = 0.52$ V, $J_{sc} = 17.4$ mA cm^{-2} and an efficiency of 6.4%. The efficiency was limited by series resistance effects on the fill factor. The quantum efficiency of these cells was panchromatic reaching values of over 90%.

The measurement of the *J–V* dependence as a function of temperature gave results similar to those of Mitchell [28] as described above, and as shown in Fig. 2. The value of J_0 at room temperature was 3×10^{-9} A cm^{-2} (increasing by a factor of about 2 under illumination), and it had a high temperature activation energy of 0.67 eV. Above room temperature the temperature dependence of the *J–V* curves indicated a recombination transport mechanism with $A = 1.45$, indicating recombination either through levels in the depletion region displaced from midgap or through interface states. Below room temperature a tunneling mechanism was indicated with $a = 28.5$ V^{-1} which could be described by the tunneling model of Riben and Feucht [36] provided that an acceptor density of 4×10^{17} cm^{-3} at the interface was assumed instead of the bulk density of about 10^{16} cm^{-3}.

The *J–V* curves for In/CdTe/graphite Schottky barriers prepared using these CSVT CdTe films were similar to those of CdS/CdTe/graphite junctions. The fact that junction properties differed only slightly between In/CdTe polycrystalline junctions, with the CdTe deposited on graphite, and In/CdTe homoepitaxial junctions, with the CdTe deposited on single-

---

crystal C
junction
A s
the appa
with tim
indium c
on the e
indium;
heterojun
Pete
$Cd_{1-x}Te$
using bo
powders
only on t
the sour
and the
depositio
source is
the same
films wit
a thin fi
values ex
tions, an
scribed a
Chu
efficiency
CdS/CdT
CdTe fil
orated o
a copper
followed
sured at
temperat
that cells
for J_0 a
et al. [28
recombin
tunneling
results o
essentially
in the sh
in the di
tially the
et al. in
for the
reducing

crystal CdTe substrates, suggests that grain boundaries intersecting the junction do not dramatically alter the junction transport properties.

A somewhat curious degradation phenomenon was observed in which the apparent carrier density near the interface of the CdTe film decreased with time (by a factor of 2 - 3 for storage at 300 K for 2000 h) under the indium contact of an In/CdTe/graphite Schottky barrier but did not decrease on the exposed surface of the CdTe and was not due to in-diffusion of indium; a similar degradation was not observed for CdS/CdTe/graphite heterojunctions.

Peters [39] applied the CSVT technique to the deposition of $Zn_xCd_{1-x}Te$ films with controllable values of $x \leqslant 0.45$ onto graphite substrates using both polycrystalline $Zn_xCd_{1-x}Te$ and mixtures of CdTe and ZnTe powders as the source materials. The value of x in the film depends not only on the composition of the source but also on the partial pressures over the source and the deposition parameters, including the ambient pressure and the temperature difference between the source and the substrate. For depositions at low ambient pressure (300 μm) the sublimation from the source is the rate-limiting step and the value of x in the film is approximately the same as in the source; this approach allows the rapid deposition of films with controlled composition by CSVT. The open-circuit voltage for a thin film $CdS/Zn_{0.45}Cd_{0.55}Te$/graphite cell was 0.48 V, lower than the values expected for CdS/CdTe/graphite cells made under the same conditions, and expected from the fact that an increase in x increases J_0 as described above.

Chu *et al.* [15] have developed the CSVT technique to produce higher efficiency CdS/CdTe heterojunction cells with the structure glass/SnO_2/CdS/CdTe/graphite:Cu and with the parameters given in Table 1. The CdTe film was deposited by CSVT on a CdS film previously vacuum evaporated on a SnO_2-coated glass; the contact to the CdTe was made by using a copper-doped graphite paste on a surface etched with $K_2Cr_2O_7$–HNO_3 followed by annealing in hydrogen. A value of $J_0 = 10^{-9}$ A cm^{-2} was measured at room temperature with an activation energy of 0.72 eV at higher temperatures. If these data are compared with those in Fig. 2, it is seen that cells with lower values for J_0 at room temperature have higher values for J_0 activation energy. In agreement with the results of Mitchell *et al.* [28] and Anthony *et al.* [49], Chu *et al.* report junction transport by recombination, with $A = 1.60 - 1.70$ above room temperature, and by tunneling at temperatures below room temperature. Compared with the results of Anthony, for example, Chu's higher efficiency is achieved with essentially the same junction transport mechanisms but with an increase in the short-circuit current (by 1.28), a decrease in J_0 (by 6) and an increase in the diode factor A (by 1.17), the values for the fill factor being essentially the same for both cells. An apparently important step used by Chu *et al.* in their preparation technique was to include an *in situ* cleaning step for the CdS/SnO_2/glass structure in the CSVT apparatus by heating in a reducing atmosphere before depositing the CdTe; at room temperature, values for J_0 were two orders of magnitude larger for cells without *in situ* cleaning than for cells with such an *in situ* cleaning step.

5. Ion-beam doping of p-type CdTe films

The difficulty of obtaining higher hole densities in p-type CdTe films is one of the major problems associated with the use of these films in solar cells. Series resistance effects, which reduce the fill factor, are frequently associated with the bulk resistance of the films, the grain-boundary resistance and the contact resistance. All these could be reduced if hole densities in p-type CdTe films could be increased.

The experience described above for CSVT deposition of CdTe films [48, 49], *i.e.* the inability to dope from a doped source during CSVT deposition, the increase in the hole density with substrate temperature during deposition and the limitation of the hole density to a maximum of about 10^{16} cm^{-3} for depositions with the substrate at 600 °C (a maximum hole density of 10^{15} cm^{-3} for the substrate at 500 °C and 10^{14} cm^{-3} for the substrate at 400 °C) was also found in an extended investigation of the deposition of CdTe films by HWVE [53 - 55].

In addition, deliberate attempts were made using HWVE to dope CdTe films during deposition by co-evaporation of such dopants as arsenic, antimony, sodium and silver. A wide variety of preparation conditions with arsenic doping yielded films with hole densities not substantially different from those obtainable without arsenic being present. For the temperature of the antimony source increasing by only a few degrees above 540 °C, an abrupt transition takes place between no doping (resistivity, 10^7 Ω cm) and a high conductivity state (resistivity, 0.1 - 1.0 Ω cm). Attempts to dope with sodium using NaCN gave results similar to those using antimony. Attempts to dope with silver suggested the possible formation of Ag_2Te with undesirable effects on film properties. In brief, all attempts to dope p-type CdTe films during deposition by HWVE were unsuccessful. This failure may be attributed to a variety of causes: (1) small sticking coefficients for the dopants on the growing surface of CdTe at elevated temperatures; (2) the evaporation of many of these dopants as molecular species such as As_4 or Sb_2 with high dissociation energies; (3) the possibility of self-compensation in CdTe; (4) the possibility of impurities being incorporated on more than one site, giving rise to amphoteric behavior and other complexities.

Chu *et al.* [56] have reported success in doping p-type CdTe films deposited on non-crystalline substrates from the direct combination of the elements in a gas flow system (CVD); using PH_3 or AsH_3, they found minimum resistivities of between 200 and 400 Ω cm for CdTe films deposited on mullite, which, coupled with a Hall mobility of 5 - 10 cm^2, indicate a maximum hole density of about 6×10^{15} cm^{-3}. Two other successes have been achieved recently in the doping of p-type epitaxial CdTe films. Using organometallic chemical vapor deposition growth with AsH_3 as the dopant, Ghandhi *et al.* [57] obtained hole densities of 2×10^{17} cm^{-3} in epitaxial films grown on single-crystal CdTe substrates at 350 °C. Bicknell *et al.* [58] obtained carrier densities of 5×10^{16} cm^{-3} using photon-assisted doping with antimony for molecular beam epitaxial growth on CdTe substrates.

Increasing the energy and chemical reactivity of component species by ionization during deposition is a technique much used for enhancing the structural and electronic characteristics of films [59, 60]. Fahrenbruch *et al.* [61] have applied these techniques to the ion-beam doping of p-type CdTe films during deposition by vacuum evaporation onto single-crystal p-CdTe, single-crystal n-CdTe and BaF_2 substrates using a range of ion-beam currents from 10^{-3} to 10 μA cm^{-2}, a range of ion-beam energies from 10 to 300 eV, and substrate temperatures from 300 to 500 °C. For a substrate temperature of 400 °C without ion-beam doping, p-type CdTe films are produced with a hole density of about 10^{14} cm^{-3}, consistent with expectations from previous CSVT and HWVE deposition experiments.

Clear evidence for doping with arsenic or phosphorus ions has been obtained with a monotonic increase in the hole density (obtained as the zero-bias value of the ionized acceptor density from capacitance *vs.* voltage measurements) for increasing ion flux and a maximum of about $(5 - 8) \times 10^{16}$ cm^{-3} for arsenic (corresponding to about 0.5% - 1% of the impinging arsenic ions being electrically active) and about 10^{17} cm^{-3} for phosphorus. A rather sharp maximum in the hole density occurs for ion fluxes between 0.2 and 2 μA cm^{-2}, with a rapid decrease to 10^{15} cm^{-3} for higher ion fluxes. There is some tendency for the hole density to increase with increasing ion energy between 10 and 50 eV, decreasing somewhat for ion energies above 100 eV. It is known from the above-cited work of Chien [47] that ion-induced damage starts to become important at about 100 eV. Films deposited with high ion fluxes or high ion energies show evidence of being damaged, the films having a large density of deep states. To establish that authentic doping had occurred, experiments were carried out with ion-beam fluxes of argon; a negligible increase in the hole density was observed.

6. Electrical contacts to p-type CdTe

Since no metal has a work function larger than the work function of p-type CdTe, a problem exists in forming low-resistance ohmic contacts at the most fundamental level. The normal alternative to forming low-resistance tunneling contacts by high doping of the CdTe surface is not immediately available because of the normal difficulties in doping p-type CdTe to high hole densities. Reviews of low-resistance contacts to p-type CdTe have been given by Ponpon [62] and Fahrenbruch [63].

Two techniques appear to be particularly useful for producing low-resistance contacts: (1) the use of a suitable etchant, usually involving potassium dichromate to prepare the surface, and (2) the use of a particular high diffusivity impurity such as lithium. An alternative possibility is the use of a high conductivity p-type buffer layer, such as ZnTe or CdHgTe, between the CdTe and the metal contact [23].

Gu *et al.* [64] described a low-resistance contact consisting of gold on a surface etched with $K_2Cr_2O_7$–H_2SO_4 but did not report any values for the contact resistivity. Jager and Seipp [65] reported that an electroless Ni–Au contact on a surface etched with $K_2Cr_2O_7$–H_2SO_4 gave a contact resistivity as low as 0.07 Ω cm^2. Anthony *et al.* [66] investigated the character and the properties of various metals on chromate-etched p-type CdTe, and concluded that a CuAu alloy on a surface etched with $K_2Cr_2O_7$–H_2SO_4 gave the best contact of this type. The contact resistivity of such a contact on p-type CdTe (resistivity, 0.5 Ω cm) is between 0.1 and 0.5 Ω cm^2 at room temperature, increasing approximately linearly with increasing CdTe resistivity. The contact resistivity increases on heating but is stable at room temperature for at least several months. If the sample is cooled, the contact resistivity increases rapidly below 300 K to values of 10^6 Ω cm^2 at 120 K.

Transport properties of the CuAu/CdTe contact were investigated by measuring the temperature dependence of *J–V* curves. It was found that these contacts could be described by the same kind of thermally assisted tunneling model discussed above for heterojunction transport, with a barrier height of 0.60 eV. Auger analysis indicated that the chromate etching produces a tellurium-rich surface that plays a key role in determining subsequent contact properties. XPS studies on chromate-etched surfaces by Haering *et al.* [31] indicated that the depletion of cadmium from the surface is much more severe than in the case of Br_2–MeOH etching and that almost half of the excess tellurium is oxidized to TeO_2 in the etching process itself.

Although these contacts are serviceable, it is evident that they are far from ideal, particularly with regard to the low temperature behavior. Lee and Bube [67, 68] have shown that contacts to p-type CdTe with very low contact resistivities down to liquid nitrogen temperature can be prepared by diffusion of lithium into the CdTe (*n*-butyllithium or vacuum-deposited lithium being the source of lithium) before evaporation of gold as the contact metal. Aven and coworkers [69, 70] had previously used lithium nitrate as a diffusion source for acceptor doping in making contacts to p-type CdTe and ZnTe. The best contact has a resistivity of 2.1×10^{-3} Ω cm^2 at 300 K and 3.7×10^{-2} Ω cm^2 at 77 K, the lowest values reported to date for p-CdTe [64, 71, 72], as shown in Fig. 3. Diffusion produces a surface hole density of about 10^{19} cm^{-3} at room temperature. The high diffusivity of lithium results in a degradation of the contacts even at room temperature, the degradation rate being critically dependent on the temperature used for the lithium diffusion. The optimum diffusion temperature appears to be about 280 °C; contacts formed on surfaces diffused with

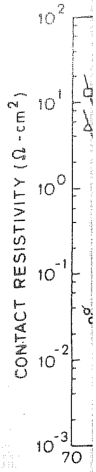

Fig. 3.
before g
5×10^7
cm); ○,
contact
ref. 68).

lithium
10^{-2} Ω

A
of the
ture o
surface
J–V cu
peratu
states a

Ackno

Th
the Ma
ment o
ciates a

Referen

1 R. F
2 D. d
3 P. R

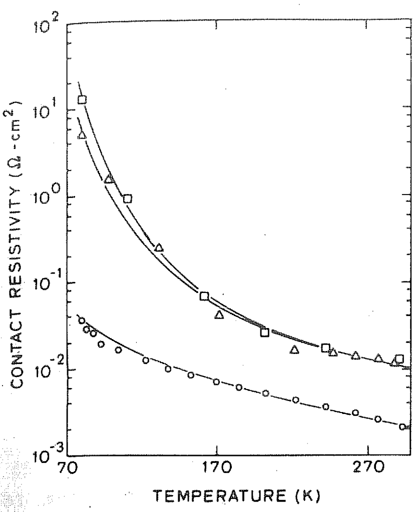

Fig. 3. Contact resistivities of Au/CdTe contacts after diffusion with *n*-butyllithium before gold deposition: □, diffusion at 330 °C for 3 min into n-type CdTe (resistivity, 5×10^7 Ω cm); △, diffusion at 330 °C for 3 min into p-type CdTe (resistivity, 3 - 10 Ω cm); ○, diffusion at 310 °C for 3 min into n-type CdTe (resistivity, 10^4 Ω cm). Calculated contact resistivities from an MIS model for the contacts are plotted as solid lines (see ref. 68).

lithium at this temperature showed a contact resistivity at 300 K of 2.5×10^{-2} Ω cm^2 after 5 months.

An MIS model has been applied to these Au/CdTe:Li contacts in view of the result of a surface analysis which indicates that the crystalline structure of the CdTe surface has been greatly disturbed and a tellurium-rich surface layer produced. This model successfully describes the measured *J–V* curves and the observed variation in the contact resistivity with temperature, the interfacial layer having a thickness of 26 Å and interface states a density between 5×10^{13} and 2×10^{14} eV^{-1} cm^{-2}.

Acknowledgments

The research at Stanford described in this paper was supported by the Materials Science Program, Division of Basic Energy Sciences, Department of Energy and the Solar Energy Research Institute. The author appreciates a critical review of this manuscript by Dr. Alan L. Fahrenbruch.

References

1 R. Frerichs, *Phys. Rev.*, *72* (1947) 594.
2 D. de Nobel, *Philips Res. Rep.*, *15* (1959) 361.
3 P. Rappaport, *RCA Rev.*, *20* (1959) 373.

4 J. J. Loferski, *J. Appl. Phys.*, *27* (1956) 777.

5 A. J. Strauss, *Rev. Phys. Appl.*, *12* (1977) 167.

6 F. V. Wald, *Rev. Phys. Appl.*, *12* (1977) 277.

7 K. Zanio, in R. K. Willardson and A. C. Beer (eds.), *Semiconductors and Semimetals, Vol. 13: CdTe*, Academic Press, New York, 1978.

8 R. H. Bube, in J. A. Amick, V. K. Kapur and J. Dietl (eds.), *Proc. Symp. on Materials and New Processing Technologies for Photovoltaics*, Electrochemical Society, Pennington, NJ, 1983, Vol. 83-11, p. 359.

9 J. Mimila-Arroyo, Y. Marfaing, G. Cohen-Solal and R. Triboulet, *Sol. Energy Mater.*, *1* (1979) 171.

10 M. Barbe, F. Bailly, D. Lincot and G. Cohen-Solal, *Proc. 16th IEEE Photovoltaic Specialists' Conf., San Diego, CA, 1982*, IEEE, New York, 1982.

11 J. G. Werthen, A. L. Fahrenbruch, R. H. Bube and J. C. Zesch, *J. Appl. Phys.*, *54* (1983) 2750.

12 Y.-S. Tyan and E. A. Perez-Albuerne, *Proc. 16th IEEE Photovoltaic Specialists' Conf., San Diego, CA, 1982*, IEEE, New York, 1982.

13 K. Yamaguchi, H. Matsumoto, N. Nakayama and S. Ikegami, *Jpn. J. Appl. Phys.*, *15* (1976) 1575.

14 K. Yamaguchi, N. Nakayama, H. Matsumoto and S. Ikegami, *Jpn. J. Appl. Phys.*, *16* (1977) 1203.

15 T. L. Chu, S. S. Chu, S. T. Ang, K. D. Han, Y. Z. Liu, K. Zweibel and H. S. Ullal, *Proc. 19th IEEE Photovoltaic Specialists' Conf., New Orleans, LA, 1987*, IEEE, New York, 1987.

16 T. Nakazawa, K. Takamizawa and K. Ito, *Appl. Phys. Lett.*, *50* (1987) 279.

17 P. V. Meyers, *Proc. Polycrystalline Thin Film Program Meet., July 20 - 22, 1987*, Solar Energy Research Institute, 1987, p. 9.

18 H. Uda, H. Matsumoto, Y. Komatsu, A. Nakano and S. Ikegami, *Proc. 16th IEEE Photovoltaic Specialists' Conf., San Diego, CA, 1982*, IEEE, New York, 1982.

19 N. Nakayama, H. Matsumoto, K. Yamaguchi, S. Ikegami and Y. Hioki, *Jpn. J. Appl. Phys.*, *15* (1976) 2281.

20 N. Nakayama, H. Matsumoto, A. Nakano, S. Ikegami, H. Uda and T. Yamashita, *Jpn. J. Appl. Phys.*, *19* (1980) 703.

21 N. Suyama, N. Ueno, K. Omura, H. Takada, S. Kitamura, T. Hibino and M. Murozono, *Proc. 19th IEEE Photovoltaic Specialists' Conf., New Orleans, LA, 1987*, IEEE, New York, 1987.

22 H. Matsumoto, K. Kuribayashi, H. Uda, Y. Komatou, A. Nakano and S. Ikegami, *Sol. Cells*, *11* (1984) 367.

23 B. M. Basol and E. S. Tseng, *Appl. Phys. Lett.*, *48* (1986) 946.

24 G. Fulop, M. Doty, P. Meyers, J. Betz and C. H. Liu, *Appl. Phys. Lett.*, *40* (1982) 327.

25 B. M. Basol, *J. Appl. Phys.*, *55* (1984) 601.

26 F. G. Courreges, A. L. Fahrenbruch and R. H. Bube, *J. Appl. Phys.*, *51* (1980) 2175.

27 J. A. Aranovich, D. Golmayo, A. L. Fahrenbruch and R. H. Bube, *J. Appl. Phys.*, *51* (1980) 4260.

28 K. W. Mitchell, A. L. Fahrenbruch and R. H. Bube, *J. Appl. Phys.*, *48* (1977) 4365.

29 Y. Y. Ma, A. L. Fahrenbruch and R. H. Bube, *Appl. Phys. Lett.*, *30* (1977) 423.

30 J. G. Werthen, J.-P. Haering and R. H. Bube, *J. Appl. Phys.*, *54* (1983) 1159.

31 J.-P. Haering, J. G. Werthen and R. H. Bube, *J. Vac. Sci. Technol.*, *A1* (1983) 1469.

32 J. G. Werthen, J.-P. Haering, A. L. Fahrenbruch and R. H. Bube, *J. Appl. Phys.*, *54* (1983) 5982.

33 J. G. Werthen, J.-P. Haering, A. L. Fahrenbruch and R. H. Bube, *J. Phys. D*, *16* (1983) 2391.

34 F. Wang, A. Schwartzman, A. L. Fahrenbruch, R. Sinclair, R. H. Bube and C. M. Stahle, *J. Appl. Phys.*, *62* (1987) 1469.

35 K. Nishimura and R. H. Bube, *J. Appl. Phys.*, *58* (1985) 420.

36 A. R
37 A. R
38 C. M
2038
39 M. G
40 C. E
Spec
41 S. J.
42 T. L.
43 J.-B.
44 F. A
Sem
45 F. A
46 M.-J.
47 K.-F
48 T. C
1296
49 T. C
(198
50 A. I
Phys
51 K. M
52 F. B
53 W. I
(198
54 T. C
17th
1984
55 R. H
C.-T.
528.
56 T. L
(198
57 S. K.
58 R. N
59 J. E.
60 J. E.
61 A. L
19th
1987
62 J. Po
63 A. L.
64 J. Gu
65 H. Ja
66 T. C
89.
67 C.-T.
68 C.-T.
69 M. A
Elect
70 M. A
71 H. T
72 M. C

36 A. R. Riben and D. L. Feucht, *Solid-State Electron.*, *9* (1966) 1055.
37 A. R. Riben and D. L. Feucht, *Int. J. Electron.*, *120* (1966) 583.
38 C. M. Fortmann, A. L. Fahrenbruch and R. H. Bube, *J. Appl. Phys.*, *61* (1987) 2038.
39 M. G. Peters, *Ph.D. Dissertation*, Stanford University, 1987.
40 C. Eberspacher, A. L. Fahrenbruch and R. H. Bube, *Proc. 17th IEEE Photovoltaic Specialists' Conf., Kissimmee, FL, 1984*, IEEE, New York, 1984, p. 459.
41 S. J. T. Owen and T. L. Tansley, *J. Vac. Sci. Technol.*, *13* (1976) 954.
42 T. L. Tansley and S. J. T. Owen, *IEEE Trans. Electron Devices*, *ED-23* (1976) 1123.
43 J.-B. Yoo, personal communication.
44 F. A. Padovani, in R. K. Willardson and A. C. Beers (eds.), *Semiconductors and Semimetals 7A*, Academic Press, New York, 1971, Chapter 2.
45 F. A. Padovani and R. Stratton, *Solid-State Electron.*, *9* (1966) 605.
46 M.-J. Tsai, A. L. Fahrenbruch and R. H. Bube, *J. Appl. Phys.*, *51* (1980) 2696.
47 K.-F. Chien, *Engineer Dissertation*, Stanford University, 1987.
48 T. C. Anthony, A. L. Fahrenbruch and R. H. Bube, *J. Vac. Sci. Technol.*, *A2* (1984) 1296.
49 T. C. Anthony, A. L. Fahrenbruch, M. G. Peters and R. H. Bube, *J. Appl. Phys.*, *57* (1985) 400.
50 A. L. Fahrenbruch, V. Vasilchenko, F. Buch, K. Mitchell and R. H. Bube, *Appl. Phys. Lett.*, *25* (1974) 605.
51 K. Mitchell, A. L. Fahrenbruch and R. H. Bube, *J. Vac. Sci. Technol.*, *12* (1975) 16.
52 F. Buch, A. L. Fahrenbruch and R. H. Bube, *J. Appl. Phys.*, *48* (1977) 1596.
53 W. Huber, A. L. Fahrenbruch, C. Fortmann and R. H. Bube, *J. Appl. Phys.*, *54* (1983) 4038.
54 T. C. Anthony, C. Fortmann, W. Huber, R. H. Bube and A. Fahrenbruch, *Proc. 17th IEEE Photovoltaic Specialists' Conf., Kissimmee, FL, 1984*, IEEE, New York, 1984.
55 R. H. Bube, A. L. Fahrenbruch, R. Sinclair, T. C. Anthony, C. Fortmann, W. Huber, C.-T. Lee, T. Thorpe and T. Yamashita, *IEEE Trans. Electron Devices*, *ED-31* (1984) 528.
56 T. L. Chu, S. S. Chu, F. Firszt, H. A. Naseem and R. Stawski, *J. Appl. Phys.*, *58* (1985) 1349.
57 S. K. Ghandhi, N. R. Taskar and I. B. Bhat, *Appl. Phys. Lett.*, *50* (1987) 900.
58 R. N. Bicknell, N. C. Giles and J. F. Schetzina, *Appl. Phys. Lett.*, *49* (1986) 1735.
59 J. E. Greene and S. A. Barnett, *J. Vac. Sci. Technol.*, *21* (1982) 285.
60 J. E. Greene, *Solid State Technol.*, *April* (1987) 115.
61 A. L. Fahrenbruch, A. Lopez-Otero, K.-F. Chien, P. Sharps and R. H. Bube, *Proc. 19th IEEE Photovoltaic Specialists' Conf., New Orleans, LA, 1987*, IEEE, New York, 1987.
62 J. Ponpon, *Solid-State Electron.*, *28* (1985) 689.
63 A. L. Fahrenbruch, *Sol. Cells*, *21* (1987) 399.
64 J. Gu, T. Kitahara, K. Kawakami and T. Sakaguchi, *J. Appl. Phys.*, *46* (1975) 1184.
65 H. Jager and E. Seipp, *J. Electron. Mater.*, *10* (1981) 605.
66 T. C. Anthony, A. L. Fahrenbruch and R. H. Bube, *J. Electron. Mater.*, *11* (1982) 89.
67 C.-T. Lee and R. H. Bube, *J. Appl. Phys.*, *54* (1983) 7041.
68 C.-T. Lee and R. H. Bube, *J. Appl. Phys.*, *58* (1985) 880.
69 M. Aven and R. K. Swank, in B. Schwartz (ed.), *Ohmic Contacts to Semiconductors*, Electrochemical Society, New York, 1969.
70 M. Aven and W. Garwacki, *J. Electrochem. Soc.*, *114* (1967) 1063.
71 H. Tews and C. An, *J. Appl. Phys.*, *53* (1982) 5339.
72 M. Chu, A. L. Fahrenbruch and R. H. Bube, *J. Appl. Phys.*, *49* (1978) 322.